HHS Public Access

Author manuscript

Mol Psychiatry. Author manuscript; available in PMC 2017 April 24.

Published in final edited form as:

Mol Psychiatry. 2017 May ; 22(5): 733–744. doi:10.1038/mp.2016.136.

Loss of hypothalamic corticotropin-releasing hormone markedly reduces anxiety behaviors in mice

Rong Zhang, PhD[1,2,3,*], **Masato Asai, MD, PhD**[1,4], **Carrie E Mahoney, PhD**[5], **Maria Joachim**[1], **Yuan Shen, MD**[1], **Georgia Gunner**[6], and **Joseph A Majzoub, MD**[1,*]

[1]Division of Endocrinology, Boston Children's Hospital, Harvard Medical School, Boston, MA 02115, USA

[2]Key laboratory of Resource Biology and Biotechnology in Western China; College of Life Science, Northwest University, Xi'an, Shaanxi, 710069, China

[3]Division for Experimental Natural Science, Faculty of Arts and Science, Kyushu University, Fukuoka 819-0395, Japan

[4]Department of Pathology, Nagoya University Graduate School of Medicine, Nagoya 466-8550, Japan

[5]Department of Neurology, Beth Israel Deaconess Medical Center, Harvard Medical School, Boston, MA 02115, USA

[6]Neurodevelopmental Behavior Core, Boston Children's Hospital, Harvard Medical School, Boston, MA 02115, USA

Abstract

A long-standing paradigm posits that hypothalamic corticotropin-releasing hormone (CRH) regulates neuroendocrine functions such as adrenal glucocorticoid release, while extra-hypothalamic CRH plays a key role in stressor-triggered behaviors. Here we report that hypothalamus-specific *Crh* knockout mice (*Sim1CrhKO* mice, created by crossing *Crh*flox with *Sim1*Cre mice) have absent Crh mRNA and peptide mainly in the paraventricular nucleus of the hypothalamus (PVH) but preserved Crh expression in other brain regions including amygdala and cerebral cortex. As expected, *Sim1Crh*KO mice exhibit adrenal atrophy as well as decreased basal, diurnal and stressor-stimulated plasma corticosterone secretion and basal plasma ACTH, but surprisingly, have a profound anxiolytic phenotype when evaluated using multiple stressors including open field, elevated plus maze, holeboard, light-dark box, and novel object recognition task. Restoring plasma corticosterone did not reverse the anxiolytic phenotype of *Sim1CrhKO* mice. *Crh*-Cre driver mice revealed that PVHCrh fibers project abundantly to cingulate cortex and the nucleus accumbens shell, and moderately to medial amygdala, locus coeruleus, and solitary

*To whom correspondence should be addressed. Rong.Zhang@childrens.harvard.edu; Joseph.Majzoub@childrens.harvard.edu.

SUPPLEMENTARY INFORMATION

Supplementary information is available at the Molecular Psychiatry website.

CONFLICT OF INTEREST

The authors declare no conflict interest.

tract, consistent with the existence of PVHCrh-dependent behavioral pathways. Although previous, nonselective attenuation of CRH production or action, genetically in mice and pharmacologically in humans, respectively, has not produced the anticipated anxiolytic effects, our data show that targeted interference specifically with hypothalamic Crh expression results in anxiolysis. Our data identify neurons that express both *Sim1* and *Crh* as a cellular entry point into the study of CRH-mediated, anxiety-like behaviors and their therapeutic attenuation.

INTRODUCTION

The stress response consists of a complex array of neuroendocrine, physiologic and behavioral adaptive/maladaptive changes that are initiated as a means of restoring stability in the face of challenge, and may lead to anxiety and depression.[1] Stress-stimulated corticotropin-releasing hormone (CRH) release is essential for coordinating the neuroendocrine and behavioral responses to stress.[2–5] Stressors activate the release of CRH from medial parvocellular paraventricular nucleus (mpPVH) neurons, which triggers pituitary release of adrenocorticotropic hormone (ACTH) and resultant secretion of glucocorticoids.[6, 7] Stress, and stress-associated dysfunction of CRH neuronal circuitries and the HPA axis in particular, have been implicated in the onset and maintenance of specific psychiatric disorders such as major depression and anxiety disorders.[8–10]

It has become increasingly feasible to explore the mechanisms underlying anxiety disorder using gene-manipulation strategies in animals.[11, 12] Global *Crh*-deficient mice confirmed the importance of Crh in neuroendocrine,[13] but not behavioral stress responses[14, 15] while mice with generalized overproduction of Crh, including in brain, exhibit heightened anxiety-like behaviors.[16] *Crhr1*-deficient mice demonstrated a robust role for Crh or a related ligand to mediate anxiety-like behaviors[17, 18] whereas a role for Crhr2 in decreased anxiety behaviors has been described,[19] but is less certain.[12]

Although CRH arising in the PVH has been assumed to play an essential role in neuroendocrine regulation of the HPA axis, its role in stress-related behaviors has not been fully studied, despite the PVH being the major brain site of CRH synthesis, with projections to many extra-hypothalamic sites involved in behavior.[20–22] We therefore selectively deleted PVH *Crh* in mice, by generating mice with *Crh* flanked by LoxP sites (*Crh*flox mice), and breeding these to *Sim1*Cre driver mice to create *Sim1Crh*KO mice.[23] *Sim1* is expressed predominantly within the PVH, the lateral olfactory tract, the supraoptic and posterior hypothalamic nuclei, with limited expression in some other hypothalamic areas and amygdala.[23, 24] Within the PVH, we found that *Crh* expression was completely abolished in *Sim1Crh*KO mice, but that in other areas such as amygdala, cerebral cortex and hippocampus, CRH expression was maintained, allowing us to dissect the roles of PVH Crh in HPA axis and stress behavior regulation. We found that hypothalamic Crh has a major role not only in the circuits controlling HPA axis responsiveness, but also in the regulation of anxiety behaviors. The anxiolytic behaviors caused by disruption of PVHCrh in *Sim1Crh*KO mice persisted after restoration of corticosterone, indicating that these behaviors were not due to the reduction in glucocorticoids in these mice. These data provide a cellular entry point into the study of Crh-mediated anxiety and its therapeutic attenuation.

MATERIALS AND METHODS

Creation of *Crh*flox (*Crh*$^{fl/fl}$) mice

*Crh*flox mice were generated using previously published methods.[25] We used homologous recombination/recombineering in embryonic stem (ES) cells to generate a modified *Crh* allele (*Crh*flox) in which exon 2, coding for Crh protein domain, is flanked by two LoxP sites (Fig. 1). Incorporation of the targeting vector into the proper genomic locus in transfected ES cells was validated using a long PCR strategy (5′ incorporation) or Southern blot analysis (3′ incorporation) (Fig. S1a, b). Incorporation-verified targeted ES cells (*neo* positive) were micro injected into C57BL/6 blastcysts, which were surgically implanted into pseudo-pregnant ICR foster female mice. Chimeric animals were mated with *Flpe*-expressing mice to remove the *neo* cassette *in vivo*. *Crh*flox mice were crossed with mice that expressed Cre recombinase under the control of either the *EIIa* promoter (B6. FVB-Tg [EIIa-Cre] C5379Lmgd/J, #003724, Jackson Laboratories), or the *Sim1* promoter (B6.FVB (129×1)-Tg [sim1-cre] Lowl/J, #006451, Jackson laboratories, which we termed *Sim1Crh*WT) to create either germline homozygous global *Crh*KO (*Crh*dl/dl) mice or PVH-specific *Sim1Crh*KO mice, respectively. Excision of exon 2 of *Crh* was confirmed using PCR. In behavioral experiments, either wildtype (WT), heterozygous *Sim1Crh*WT, or homozygous *Crh*flox male mice were used as controls, as indicated. All mice were on a C57BL/6 background, and were between 12 and 40 weeks of age. Animals in different groups of each experiment were within 2 weeks of age.

All the required plasmids (PL253, PL452, and PL451) and recombinogenic bacteria strains (EL350) were obtained from Dr. David Conner (Harvard Medical School Department of Genetics). The 129Sv BAC clone (bMQ-297H8) containing the mouse *Crh* gene (accession# NM_205769) in DH10B was obtained from Sanger Institute (http://www.sanger.ac.uk/). BAC DNA was extracted and transferred to recombinogenic *E.coli* (EL350). Primers were designed to create miniarms for PL253 to retrieve the mouse CRH gene and its flanking regions (PL253_44705FNOT/PL253_45104RXBA and PL253_57935FXBA/PL253_58229RBAM), miniarms for PL452 for the upstream loxP insertion (PL452_49460FSAL/PL452_49859RECO and PL452_49860FBAM/PL452_50259RNOT) and miniarms for PL451 for the downstream FRT-Neo-FRT-LoxP insertion (PL451_51214FSAL/PL451_51613RECO and PL451_51614FBAM/PL451_52103RNOT). To utilize endogenous XbaI sites (TCTAGA) for retrieval, the XbaI site on PL253 plasmid was destroyed using DNA polymerase I, Large (Klenow) Fragment (New England Biolabs, MA) before ligation, which was named‘PL253delXba’. Two PCR-amplified, subcloned, and sequence-verified miniarm fragments for (PL253delXba, PL452, and PL451) were ligated with the designated vector at (NotI/XbaI/BamHI, SalI/EcoRI/BamHI/NotI, and SalI/EcoRI/BamHI/NotI), respectively. PL253delXba with miniarms was digested with XbaI, underwent electroporation into the BAC in EL350 and was selected with ampicillin to retrieve a 13.5 kb genomic DNA fragment containing the mouse *Crh* gene. PL452 with miniarms was digested with SalI/NotI/ScaI to obtain a 2.7 kb fragment, which underwent electroporation into EL350 containing the retrieved vector and was spread on LB kanamycin plates to introduce the floxed Neomycin cassette. The PL253delXba fused with PL452 was introduced into Arabinose-treated EL350 to remove the floxed Neomycin cassette. In a like manner, PL451

with miniarms was digested with SalI/NotI/ScaI to obtain a 2.7 kb fragment, which underwent electroporation into EL350 containing the upstream-loxP introduced vector and was spread on LB kanamycin plate to introduce the second loxP site to obtain the final targeting vector. The final targeting vector was verified by functional testing (Flpe induction in EL250 or Cre induction in EL350), restriction enzyme digestion, and DNA sequencing. The final targeting vector was linearized with NotI, electroporated into 129Sv ES cells and selected with G418 (Invitrogen).

Incorporation of targeting vectors into the proper genomic loci in transfected ES cells was validated using a long PCR strategy (5′ incorporation) or Southern blot analysis (3′ incorporation) (Fig. S1a, b). Briefly, G418 resistant ES cell lines were isolated and analyzed with long PCR using LA Taq (TAKARA BIO INC. Otsu, Japan), external primer and internal primer at both 5′ and 3′ ends to confirm both 5′ and 3′ incorporation of the construct into the proper genomic loci. Long PCR products were 6443 bp using CRH5PextF1_LA and PL452whole98bpR, and 8492 bp using CRH5PextF1_LA and NeoRev3. Long PCR products were cloned into TOPO-XL vector (Invitrogen) and verified with sequencing. Southern blot analysis was carried out using a ^{32}P-labeled 3′probe and genomic DNA extracted from ES cells. Briefly, the 3′ probe was designed for the specific region of DNA external to the construct to confirm site-specific genomic targeting. BamHI digested genomic DNA was electrophoresed on 0.75 % agarose gel in 1xTBE buffer, transferred to a Nylon membrane, and hybridized with probe. After the membrane was washed, bands were visualized using a phosphor screen.

Primer sequences

1. Constructing primers

PL253_44705FNOT 5′-GCGGCCGCATTTGCCCTGGAGGGAAAGGAG-3′

PL253_45104RXBA 5′-TCTAGAACTATATCATCATAAAAT-3′

PL253_57935FXBA 5′-TCTAGAAGCTAAGTGAAATG-3′

PL253_58229RBAM 5′-GGATCCAAACCAAGTTGTGCCAGGGA-3′

PL452_49460FSAL 5′-GTCGACTTGAGAGACTGAAGAGAAAG-3′

PL452_49859RECO 5′-GAATTCTGGGATGCAATAGGGGAGCC-3′

PL452_49860FBAM 5′-GGATCCTGTCCCCAAGCAAACGGAGT-3′

PL452_50259RNOT 5′-GCGGCCGCAGGTCGGGGGAGAGAGAAGG-3′

PL451_51214FSAL 5′-GTCGACCATTCTTGAGGGGTGGCTAG-3′

PL451_51613RECO 5′-GAATTCTTTAGAGGTGGGAGGAACCTC-3′

PL451_51614FBAM 5′-GGATCCACTTGATCACAGTGGAAATAAC-3′

PL451_52013RNOT 5′-GCGGCCGCGCAAACGTATTAAAATTAGAAG-3′

2. Long PCR primers

CRH5PextF1_LA 5′-CCAGAGGAGTGGGGCTTGTCAGAGAACTGGACACA-3′

PL452whole98bpR 5′-GGATCCCCTCGAGGGACCTAATAACTTCGTATAGCATACATTATACGAAGTTATATTAAGGGTTATTGAATATGATCGGAATTGGGCTGCAGGAATTC-3′

NeoRev3 5′-GGGAACTTCCTGACTAGGGGAGGAGTAGAAGGTGG-3′

3. Primers for southern probe

3P external_F 5′-AAGCAGAAATGTGCTTGTGTG-3′

3P external_R 5′-AGGGGCTGCTGAGTTAACTC-3′

4. Genotyping primers

4.1) Downstream genotyping

CRH_51359_F 5′-CAAAGGTTGCTGTGGCTTTATTTTTCCTCTTCA-3′

CRHNeo_F 5′-ATGGCTTCTGAGGCGGAAAGAACCA-3′

CRH_51706_R 5′-TTGTCCTCTGACCTCCACCCACTTC-3′

4.2) Flpe genotyping (Flpe 725 bp, internal control WT 324 bp)

Flpfwd (IMR1348) 5′-CACTGATATTGTAAGTAGTTTGC-3′

Flprev (IMR1349) 5′-CTAGTGCGAAGTAGTGATCAGG-3′

IMR0042 5′-CTAGGCCACAGAATTGAAAGATCT-3′

IMR0043 5′-GTAGGTGGAAATTCTAGCATCATCC-3′

4.3) Upstream genotyping

CRH_49667_F 5′-CCAGCTGCCCATGTGCTGGA-3′

CRH_49959_R 5′-CGCACACCCTAATCGCCCCC-3′

Corticosterone treatment

Because loss of PVHCrh reduces plasma corticosterone, which might independently affect behavior in *Sim1Crh*KO mice, some animals were administered corticosterone in their drinking water to restore the plasma corticosterone towards normal (*Sim1CrhKO*Cort). Corticosterone (Sigma-Aldrich, #C2505) was initially dissolved in ethyl alcohol and diluted to a final concentration of 5 or 10 ug/ml in water (0.2% ethyl alcohol final concentration). Control *Crh*flox mice were randomly assigned to receive either drinking water with 0.2% ethyl alcohol (*Crh*floxCon), or drinking water with corticosterone (*Crh*floxCort).

Tail blood collection

We collected tail blood (~10ul) in the morning (7–9 am) or evening (5–7 pm) as previously described.[26] Within 60 seconds after removal from the home cage, blood was collected from a small ventral incision near the tail tip by gently milking the tail to deliver ~10ul blood into EDTA-coated microvette tubes. Mice were immediately released back to their home cages after bleeding.

Behavioral tests and data analysis

Adult male mice were housed individually. Animals were maintained on a 12 h light/dark cycle in a temperature- and humidity- controlled vivarium, with lights on from 7 am to 7 pm. Animals were maintained in accordance with the National Institutes of Health Guide for the Care and Use of Laboratory Animals (1996). All animal procedures were approved by the animal research facility at Boston Children's Hospital and Harvard Medical School. All behavioral tests were performed in our neurodevelopmental behavior core (http://core.iddrc.org/neurodevelopmental-behavioral) laboratory in an isolated test room under low light conditions (≈30 lumens). Animal's behaviors were recorded with an overhead Panasonic WVBP334 digital camera, and video tracking was done with Noldus Information Technology Ethovision XT9 software (Noldus Information Technology, Wageningen, Netherlands). Only one behavior test was performed per day starting at 9 am. Between sessions, the maze/field/arena was rinsed with water and dried with paper towels. All behavioral measurements were calculated using the Ethovision program XT9 and manually analyzed by an observer blinded to genotype and treatment.

Shirpa test—Shirpa test screening was conducted to determine whether *Sim1Crh*KO mice have normal physiological functions prior to performing anxiety testing. This screen covers a variety of physiological and behavioral assessments including muscle and lower motor neuron, spinocerebellar, and sensory functions.[27] Animals received a score for each measured behavior and position, and total scores were analyzed. Animals were scored in a viewing jar for body position (0=active; 1=inactive; 2=excessive activity), tremor (0=present; 1=absent), palpebral closure (0=present; 1=absent), coat appearance (0=normal; 1=abnormal), whisker (0=present; 1=absent), lacrimation (0=present; 1=absent), and defecation (0=present; 1=absent). Mice were then transferred to an arena, where we scored transfer arousal (0=extended freeze; 1=brief freeze; 2=immediate movement), gait (0=fluid movement; 1=lack of fluidity), tail elevation (0=dragging; 1=horizontal extension; 2=elevated tail), startle response (0=prayer reflex; 1=absent; 2=reaction in addition to reflex), touch escape (0=none; 1=response to touch; 2=flees prior to touch), positional passivity (0=struggles when held by tail; 1=struggles when scruffed; 2=struggles when laid supine; 3=no struggle), skin color (0=pale; 1=pink; 2=red), trunk curl (0=present; 1=absent), limb grasping (0=present; 1=absent), visual placing (0=present; 1=absent), righting reflex (0=present; 1=absent), pinnal reflex (0=present; 1=absent), contact righting reflex (0=present; 1=absent), corneal reflex (0=present; 1=absent), biting (0=present; 1=absent), vocalization (0=present; 1=absent), morphology (0=normal; 1=abnormal), tail pinch (0=response; 1=no response), and pupillary light reflex (0=present; 1=absent).

Restraint—Restraint was performed by confining mice in ventilated conical tubes (Corning, NY) to inhibit movement for 30 minutes.[28] Tail blood was collected prior to restraint (0 minutes), immediately after the termination of restraint (30 minutes), and at 3 later time points (60, 120, and 240 minutes from the initiation of restraint).

Open Field Test—The open field test was modified as described.[29] In this test, the time spent in each zone (center, neutral and wall) and distance traveled in these areas were calculated. Our open-field apparatus consisted of a 45cm diameter circular arena, which was divided into 3 zones (center, neutral and wall), each defined as 1/3 the diameter of the arena (15cm). Each mouse was placed toward the wall at the 6 o'clock position of the open field. Each trial lasted for 15min, with one trial per mouse. Time spent in the different zones, latency and frequency entering into different zones, and total traveled distance were analyzed.

Holeboard Test—The holeboard apparatus consists of 16 (4 × 4) holes in a square arena (42 ×42 cm) with 16 × 16 photo beams for locomotor activity and 1 photo beam in each hole for exploratory behavior. Mice were placed gently at the 6 o'clock position to allow them to explore the arena for 15 minutes. The number of center area entries, distance moved in the periphery and center, and time spent in the periphery and center area were calculated. Fine movement, and head/body stretch and movement (which are considered as subtle risk assessment measures) were scored. Fine movement was calculated as the number of single beam breaks the animal made repeatedly (e.g., moving its head from left to right and back again).[30]

Elevated Plus Maze (EPM)—The EPM test was modified as previously described.[31] The apparatus consisted of a black melamine central square platform (76 × 76 cm) from which four black melamine arms radiated: two oppositely positioned open arms (76×7cm) and two oppositely positioned enclosed arms (76×7cm). The maze was elevated to a height of 74cm from the floor and indirectly illuminated (light intensity in open arms: 25–30 lux). Mice were placed individually into the central platform facing toward an open arm and allowed 6 min of free exploration of the apparatus. An arm entry was defined as the entry of all four paws into one arm. The following dependent variables were measured: time spent in open/closed arms and center, percentage of time spent in each area, number of open/closed arm entries, total distance traveled and velocity.

Light-Dark Box—The light-dark box apparatus consisted of 2 rectangular compartments (26 × 26 cm) connected by a door.[32] One compartment is white and illuminated (80 lux), and the other is black and dark (0 lux). Mice were placed gently in the center of the dark area facing the door for 5 minutes, the latency to the first entry in the light area, the number of entries, and the percentage of time spent in the light area, total moved distance and velocity were measured.

Novel Object Recognition Task (NORT)—The NORT test has been introduced into anxiety testing recently, although it was originally developed to assess non-spatial working memory.[33–36] In the present study, the modified protocol consisted of 2 sessions. In the training session, mice were presented with two identical objects (2 small white p.v.c pipes

with screws) in the square arena (W20 × L20 × D10 cm) and allowed to explore them for 5 min (same object trial). Animals were returned to their home cages for a 5 min break. Then, one of the two familiar objects was replaced with a novel object (1 blue glass cylinder for novel object) and the mice were again allowed to explore them for 5 min (choice trial). The novel object was randomly placed into either the left or right test arena. The animal was considered to be "investigating" an object when its nose-point, detected by Noldus Information Technology Ethovision XT9 tracking software, entered into the designated zone containing the object. The cumulative duration for familiar object, novel object, frequency to either object, total distance traveled and velocity were calculated by the program.

All behavioral tests were performed in three different animal models. First, the behavioral effects of *Sim1*Cre and *Crh*flox were assessed by comparing *Crh*WT, *Sim1Crh*WT, and *Crh*flox mice. Next, the effect of removing Crh from Sim1 neurons on anxiety behaviors was investigated in *Sim1Crh*KO compared with *Crh*flox mice. Finally, to differentiate the effect of loss of PVHCrh from reduced corticosterone in *Sim1Crh*KO mice, behavioral testing was performed in *Sim1Crh*KO and *Crh*flox animals treated with corticosterone (5–10ug/ml) or vehicle in drinking water, as described above.

Radioimmunoassays (RIA)

Plasma concentration of corticosterone and ACTH were determined by radioimmunoassay using ^{125}I RIA kits from MP Biomedicals.[37] All corticosterone plasma samples were analyzed in duplicate, and plasma corticosterone measures from a single experiment were performed in the same RIA analysis to avoid interassay variability. For ACTH, single plasma samples were analyzed due to the large required volume (50 ul of plasma/mouse). We performed several experiments using different cohorts of mice with similar results in all experiments.

In situ hybridization (ISH)

In situ hybridization was performed as described previously.[37, 38] Brains were collected with isopentane on dry ice and stored at −80°C. Targeted brain areas (from Bregma −0.10 to Bregma −1.70) were sectioned (12um) onto coated slides from coronal direction according to the Mouse Brain in Stereotaxic Coordinates.[39] Antisense cRNA probes complementary to mouse *Crh* exon 2 (578 bp) were used for in situ hybridization. The *Crh* DNA construct was subcloned into pGEM4Z vector (Promega), linearized with HindIII, and transcribed with SP6 RNA polymerase. The probe was labeled by in vitro transcription using [^{35}S] UTP, with prehybridization, hybridization, and post-hybridization protocols conducted as described previously.[37, 38] Hybridized slides were exposed on Kodak Biomax MR-2 film (Eastman Kodak) for 5 days. Images were captured from epson scanner (epson perfection V700 photo; Epson, USA). *Crh*KO mice were included as specificity negative controls. Assessment of PVH Crh mRNA expression was performed using the Mouse Brain in Stereotaxic Coordinates.[39]

Semi-quantitative analysis was conducted on every sixth brain section containing the anatomical region of interest using NIH Image software (http://imagej.nih.gov/ij/). The average gray level (signal) was quantified bilaterally in the PVH by subtracting the gray

level signal over a non-hybridized area of tissue (white matter) and expressed as the corrected gray level. The mean corrected gray level values were calculated for each animal and used in the statistical analysis in a blinded manner.

Q-RT-PCR

Animals were euthanized by cervical dislocation and brains were rapidly removed. PVH and brainstem were collected using a cooled mouse brain matrix with 0.5mm section dividers (ASI Instruments Inc., Warren, MI). Using the Palkovits punch technique (Electron Microscopy Science, PA), PVH was dissected using the fornix, optic tracts, and third ventricle as landmarks (Bregma, around −0.22mm to −1.70mm). Samples from different animals of the same genotype were pooled together to extract RNA. NTS-enriched brainstem was isolated from the anterior (rostral) margin (Bregma −6.12mm), to the posterior (caudal) margin (Bregma −8.12) using obex (bregma, −3.8mm) and the fourth ventricle as previously published.[40] Whole hypothalamus was isolated by block dissection according as previously described.[41] The landmarks including the fornix (Bregma, −0.22mm), optic tracts and mammillary nuclei (Bregma, −2.54mm) were used to dissect the hypothalamic region. Collected tissues from animals were transferred into RNAlater, and total RNA was extracted using RNeasy Plus Universal kits (Qiagen). cDNAs were synthesized (SuperScriptTM III First-Strand Synthesis System; Invitrogen) according to the manufacturer's instruction. Q-RT-PCR was performed as previously described.[37] *Crh* primer sequences were designed using Primer3 software[42] and synthesized by IDT. Q-RT-PCR analysis was performed in the iCycler iQ Multi-Color Real Time PCR Detection System (Bio-Rad). cDNA amounts present in each sample were determined using iQ SYBR Green Supermix (Bio-Rad). Threshold cycle readings for each of the unknown samples were used, and the results were calculated in Excel using the ΔΔCt method, using L32 as a house-keeping reference gene.[43] Negative RT samples were included to rule out genomic DNA contamination.

Q RT-PCR primers:

CRH_F 5′- TCTGCAGAGGCAGCAGTGCGGG -3′

CRH_R 5′- CGGATCCCCTGCTGAGCAGGGC -3′

L-32_F 5′- GCCAGGAGACGACAAAAA -3′

L-32_R 5′- AATCCTCTTGCCCTGATCC -3′

Immunohistochemistry (IHC)

Free-floating sections were incubated with a rabbit anti-Crh antibody (diluted 1:5000; a generous gift from the late Dr. Wylie Vale's lab) overnight at 4°C and Crh IHC staining was performed as described previously.[37] Sections were rinsed five times for 5 min in 50mMKPBS and subsequently incubated in biotinylated goat anti-rabbit secondary antibody (diluted 1:500; Vector Laboratories) for 1 h. Following five, 5 min rinses in KPBS, sections were incubated in avidin-biotin complex (diluted 1:1000; Vector Laboratories) for 1 additional hour. Sections were rinsed five times for 5 min in KPBS, incubated in biotin-labeled tyramide (diluted 1:250; PerkinElmer Life Sciences), rinsed five times for 5 min, and

incubated in Cy3-conjugated streptavidin (diluted 1:500; Jackson ImmunoResearch) for 30 min. All sections in the series were then examined by fluorescence microscopy to identify positively labeled cells and fibers. Images of the PVH were captured from low to high magnification by using a Nikon E800 microscope and Nikon Elements software.

PVHCrh projection tracing

To track PVHCrh projections in the brain, we stereotaxically microinjected 40 nl of AAV8-FLEX-hsyn-ChR2-mCherry (UNC Vector Core) into the unilateral PVH (from bregma: A/P 0.26, M/L 0.76, D/V −4.8) of adult Crh-ires-Cre mice[44] (a gift from Dr. Bradford Lowell) using a glass micropipette and an air pressure injection system. Mice were perfused 7 weeks later, the brains were removed and stored in 10% formalin overnight followed by transfer into 20% sucrose. Sectioned brain tissue (30um) was quenched in 0.3% H_2O_2 for 30 minutes, and then incubated overnight with rabbit polyclonal antiserum against mCherry (1:5000; Clontech #632496). Between this incubation and each subsequent incubation, tissue was washed with 1XPBS for 5 min × 5 times. On the second day, sections were incubated with biotinylated-conjugated donkey anti-rabbit antiserum (1:500, Jackson#712065152) for 2 h, followed by avidin-biotin complex (ABC) solution for 1h. Sections were incubated in DAB (3, 3′-Diaminobenzidine), TBS, H_2O_2 for less than 5 minutes. Sections were mounted and coverslipped (Cytoseal, Thermoscientific). Images were captured with a Zeiss AxioCam HRc microscope and AxioVision Rel software (v4.8).

Hematoxylin and Eosin staining (HE staining)

Adrenals were collected into 10% formalin and tissues were sectioned at 6um thickness from paraffin-embedded blocks and stained with hematoxylin and eosin in the Rodent Histopathology Core lab, Harvard Medical School (http://www.dfhcc.harvard.edu/research/core-facilities/rodent-histopathology/). Images were taken and analyzed using a Nikon E800 microscope and Nikon Elements software.

Statistical analyses

Data are expressed as mean ± SEM. Data were analyzed using two-tailed Student t test for samples with similar variances, ANOVA, and repeated measures ANOVA as appropriate (Statview, SAS Institute; GB Stat version 9.0, Dynamic Microsystems). Significant main effects were analyzed by the PLSD post hoc test. Significance for all statistical analyses was set at $P \leq 0.05$. All sample sizes were determined by prior pilot studies to determine the minimum number of animals required to achieve statistical significance. No animals were excluded from analysis in any experiment.

RESULTS

Characterization of *Crh*flox and *Crh*KO mice

*Crh*flox mice (*Crh*fl/fl) were crossed with *EIIa*Cre mice to create global *Crh*KO mice (*Crh*dl/dl) (Fig. 1a; Fig. S1a, b). *Crh*flox and *Crh*WT mice revealed a similar expression pattern and comparable fluorescent density for Crh, which indicates that the insertion of loxP sites flanking *Crh* exon 2 did not affect Crh protein expression. Compared to these animals, *Crh*KO revealed the expected complete loss of Crh peptide in the PVH and CeA

(Fig. 1b–g). *Crh*flox mice had normal adrenal morphology (Fig. 1h, i), whereas *Crh*KO mice had a markedly atrophic appearance of the zona fasciculate of the adrenal gland, the area primarily responsible for basal as well as stress-triggered corticosterone release (Fig. 1j, k). Homozygous *Crh*flox mice revealed normal food intake and bodyweight (Fig. S2a, b). *Crh*KO mice born from *Crh*dl/+ heterozygous mothers had normal growth, viability and fertility without a requirement for glucocorticoid replacement. However, all offspring of homozygous *Crh*KO mothers died within the first several hours of delivery after a normal 19–20 days' gestation. These offspring showed lung dysplasia in comparison to *Crh*flox neonates at 2 h of life. *Crh*KO neonates showed marked hypercellularity of the lungs, increased alveolar thickness and paucity of air spaces in comparison to those neonates from *Crh*flox mice (Fig. 1l–q). Administration of corticosterone (30ug/ml in drinking water) to pregnant *Crh*KO mothers fully reversed *Crh*KO neonates' death with resulting normal lung morphology (Fig. 1p, q).

*Crh*flox mice showed comparable morning and evening plasma corticosterone compared to *Crh*WT mice indicating a normal glucocorticoid diurnal rhythm. Loss of Crh in *Crh*KO mice severely reduced basal plasma corticosterone (Fig. S3a). *Crh*flox mice had a normal glucocorticoid stress response to an acute 30 min restraint challenge, which, as in WT mice, declined over time following the termination of restraint (Fig. S3b). Under these same conditions, *Crh*KO mice had reduced glucocorticoid release (Fig. S3a, b). These results are consistent with the adrenal atrophy demonstrated in *Crh*KO mice (Fig. 1h–k). In all of these ways, this *Crh*KO mouse line is a phenocopy of a previously-created line of global *Crh*KO mice,[13] which demonstrates that the Cre-loxP strategy using *EIIa*Cre targeting *Crh* exon 2 results in the complete loss of *Crh* expression and function.

Characterization of *Sim1Crh*KO mice

Analysis of Crh mRNA by in situ hybridization revealed different Crh expression patterns in *Crh*flox and *Sim1Crh*KO mice: as expected, *Sim1Crh*KO mice had markedly reduced Crh mRNA in hypothalamus, particularly in the PVH region from bregma −0.58 to bregma −1.06, consistent with co-expression of Crh and Sim1Cre in this area (Fig. 2, a–d). In contrast, Crh mRNA expression was no different between *Sim1Crh*KO and *Crh*flox mice in other areas such as central amygdala and cerebral cortex, indicating successful PVH deletion of Crh by Sim1Cre. Global *Crh*KO mice did not show any Crh mRNA signals in the brain (Fig. 2e, f). Semi-quantitation of Crh mRNA expression by in situ hybridization confirmed that Sim1Cre efficiently deleted 70~80% of Crh in PVH (Fig. 2g). Using Q-RT-PCR to measure Crh mRNA expression in *Sim1Crh*KO mice, we found a 60~70% reduction in PVH-enriched hypothalamic punches (Fig. 2h), but only a 30% reduction in whole hypothalamus (Fig. S4), and no decrease in brainstem (Fig. 2h). *Sim1Crh*KO mice revealed deceased expression of Crh-immunoreactivity in PVH compared to *Crh*flox mice (Fig. 2 i, j), consistent with the decrease in Crh mRNA (Fig. 2c, d). In contrast, Crh-immunoreactivity in CeA was similar between the two groups (Fig. 2k, l).

Loss of PVH Crh affects adrenal development and HPA responsiveness

*Sim1Crh*KO mice revealed striking adrenal atrophy, particularly in the zona fasciculata, the primary corticosterone-producing area (Fig. 2 m–p). Both adrenal weight, adjusted adrenal

weight [adrenal weight (milligrams)/bodyweight (grams) × 100] and adrenal cross-sectional area were decreased by deletion of *Crh* in Sim1 neurons (Fig. S5a).

As expected, disruption of Crh expression in PVH affected downstream pituitary ACTH secretion, as manifested by the significantly decreased plasma ACTH in *Sim1Crh*KO mice compared to control mice despite their having lower plasma corticosterone (Fig. 2q, r). Introduction of Sim1Cre did not affect basal plasma corticosterone (Fig. S5b). In addition to reduced basal plasma corticosterone in Sim1CrhKO animals (Fig. 2r), loss of PVH Crh significantly attenuated stress-induced plasma corticosterone release (about 2/3 less than control) in Sim1CrhKO animals (Fig. S5d).

General Health Characterization of *Sim1Crh*KO mice

Before analyzing more subtle behaviors, all animals were screened by a modified Shirpa test protocol for functional and physiological behavior assessment.[27] There were no differences in total Shirpa scores between control (*Crh*flox) and *Sim1Crh*KO mice, suggesting that disruption of *Crh* in Sim1 neurons does not affect overall physical and physiological characteristics (Fig. S6).

Attenuation of anxiety behaviors in *Sim1Crh*KO mice

The role of PVH CRH in neuroendocrine HPA axis regulation is clear,[13] but the site of CRH involved in the regulation of stress-associated behaviors such as anxiety is less so. Moreover, global knockout of *Crh* in mice,[14, 15] and pharmacological antagonism of CRH in humans,[45] has not produced anxiolysis. We therefore evaluated anxiety behaviors in *Sim1Crh*KO mice. In the open field paradigm, *Sim1Crh*KO mice had increased cumulative duration in the center (Fig. 3a, b). *Sim1Crh*KO animals showed shorter latency into both center and neutral areas compared to control mice, indicating that disruption of *Crh* in Sim1 neurons significantly decreased emotional anxiety behaviors (Fig. 3c). Consistent with this, deletion of *Crh* in Sim1 neurons increased the frequency of entering the center area while there were no differences for entering neutral and wall areas (Fig. 3d). Both *Sim1Crh*KO and control mice increased their time spent in the center during the last 5 minutes of testing, but *Sim1Crh*KO mice showed striking increment at the beginning (0min–5min) and middle (5min–10min) period (Fig. S7a). *Sim1Crh*KO mice more frequently entered the center area during the first 10 minutes, although eventually control mice did so as well (Fig. S7b). No differences were found in total distance travelled and velocity between *Sim1Crh*KO and *Crh*flox control mice (Fig. S7c).

The holeboard task also measures anxiety behaviors due to the reluctance of rodents to enter the center of an open arena. It provides a more subtle assessment of anxiety which may be missed in other behavioral tests because this task does not evoke a high level of arousal or fear.[46] In agreement with the open field testing, the total entries into the center of the holeboard were significantly greater in *Sim1Crh*KO mice, with differences observed during the test's first 10 minutes (Fig. 3e). *Sim1Crh*KO animals significantly increased their fine movement behaviors compared to *Crh*flox control mice in the first 10 minutes of the test, suggesting that loss of PVH Crh attenuated subtle anxiety behaviors, with the animals showing more exploratory tendency and risky behaviors in their new environment (Fig. 3f).

We did not observe any genotype differences in the time spent in both center and periphery area of the holeboard arena (Fig. S8a, b). *Sim1Crh*KO mice moved more into the center, although this difference did not reach statistical significance (Fig. S8c).

In the EPM test, we found a significant effect of genotype. The frequency of entry into the open arms was not different between genotypes but *Sim1Crh*KO animals spent less time in the closed arms, suggesting that they had increased exploratory behaviors outside of the closed arms. *Sim1Crh*KO animals significantly increased the time spent in the open arms (Fig. 4 a–c). However, we did not observe differences for duration in center or duration in closed arms on the EPM apparatus (Fig. S9). In another traditional anxiety test, the light-dark box test, *Sim1Crh*KO animals showed decreased latency to enter the lit compartment compared to the littermate siblings (Fig. 4d).

The novel object recognition test (NORT) assesses general anxiety behaviors by using familiar and novel object stimuli. *Sim1Crh*KO mice showed significant preference for approaching a novel versus a familiar object, indicating that Crh expressed in Sim1 neurons is critical to regulate anxiety activities towards new stimuli. *Sim1Crh*KO mice also exhibited decreased latency to approaching novel versus familiar objects (Fig. 4e), greater frequency of approach to novel versus familiar objects (Fig. 4f). *Sim1Crh*KO mice showed longer exploratory duration around a novel object (Fig. S10a), suggesting that *Sim1Crh*KO mice have lower anxiety toward exploring novel objects. Animals did not show any position preference in either familiar or novel objects trials, since they had similar touching/recognizing behaviors for familiar objects between groups during both same and novel object trials regardless the object positions (Fig. S10b). In contrast, we observed that *Sim1Crh*KO and *Crh*flox control mice travelled overall similar distances around novel and familiar objects (Fig. S10c), again suggesting that loss of PVH Crh did not affect their general locomotion behaviors.

As we expected, deletion of hypothalamic *Crh* attenuated stress-stimulated plasma corticosterone during the open field test (Fig. S11a), holeboard test (Fig. S11b), EPM test (Fig. S11c), light-dark-box test (Fig. S11d) and NORT behavior assessment (Fig. S11e). These data support the important role of PVH Crh in regulating the responsiveness of the HPA axis.

The results of behavioral assays were similar among *Crh*WT, *Crh*flox, and *Sim1Crh*WT mice in the open field (Fig. S12a), EPM (Fig. S12b), light-dark box (Fig. S12c), holeboard (Fig. S12d), and NORT tests (Fig. S12e). This indicates that *Sim1*Cre itself is not involved in the anxiolytic phenotype of *Sim1Crh*KO mice.

Anxiolytic behavior in *Sim1Crh*KO mice is not due to reduced plasma corticosterone

Because loss of PVHCrh reduces plasma corticosterone, which might independently affect behavior in *Sim1Crh*KO mice, we performed behavioral testing in these mice after administration of corticosterone in their drinking water to restore the plasma corticosterone towards normal (*Sim1CrhKO*Cort mice). With their nocturnal drinking pattern, *Sim1CrhKO*Cort mice exhibited a quasi-normal diurnal rhythm in plasma corticosterone, being high when measured in the early morning (after drinking during the night) and low

when measured in the early evening (after not drinking during the daytime) (Fig. 5a). Compared to *Crh*floxCon and *Crh*floxCort mice, *SimCrh*KOCort animals spent more time in the center of the open field (Fig. 5b). Compared to *Crh*floxCon and *Crh*floxCort mice, *Sim1Crh*KOCort animals entered the open arms of the EPM more frequently and for a longer duration (Fig. 5c), anxiolytic behaviors similar to those of untreated *SimCrh*KO mice (Fig. 4 a–c). Interestingly, *Crh*floxCort animals showed decreased time in the EPM open arms, suggesting an anxiogenic effect of supplemental corticosterone in these mice (Fig. 5c). In the light-dark box, *Sim1Crh*KOCort animals spent more time in light dark box although the results did not reach statistical significance (Fig. 5d). Similar to the *Sim1Crh*KO mice in the holeboard test (Fig. 3f), *Sim1Crh*KOCort mice had significantly increased fine movement (Fig. 5e). There was a nonsignificant trend of increased cumulative duration for novel object interaction in *Sim1Crh*KOCort (Fig. 5f). These results suggest that the anxiolytic behavior in *Sim1Crh*KO mice is not due to reduced plasma corticosterone.

Identification of efferent projections of PVHCrh-responsive neurons

Using an AAV reporter in a mouse expressing Cre from a *Crh* promoter driver,[44] we traced the efferent projections of PVHCrh neurons in Crh-ires-Cre mice (Fig. S13). As expected, there were intense projections of PVH Crh to the median eminence (Fig. S14i). We observed moderate to dense fiber projections to several brain areas that may be involved in anxiety behaviors, including the cerebral cortex, amygdala, septum, bed nucleus of the stria terminalis (BNST), accumbens nucleus (Acb), hypothalamus, midbrain, and brainstem, including nucleus of the solitary tract (Sol) and locus coeruleus (Fig. S14). The anatomical distribution of these and other PVH efferent projecting fibers was qualitatively analyzed (Table S1).

DISCUSSION

In this report, we have found that selective Crh deficiency in Sim1 neurons causes, as expected, 1) decreased basal ACTH and glucocorticoid plasma concentrations; 2) attenuated glucocorticoid secretion following variable stress challenges; and 3) adrenal gland atrophy, particularly in the zona fasciculata, the region responsible for corticosterone production. Unexpectedly, Crh deficiency in Sim1 neurons also causes markedly attenuated stressor-induced anxiety-like behaviors evaluated by open field,[47] holeboard,[30] elevated plus maze,[31] light-dark-box,[32] and novel object recognition task,[35] effects that were not reversed by corticosterone supplementation of *Sim1Crh*KO mice. Moreover, we found that PVHCrh fibers project widely to areas that are potentially involved in behavior, including BNST, MeA, CeA, NTS and LC. The consistency and robustness of the behavioral findings across these different test modalities that address different aspects of anxiety[48] indicate that Crh expressed in Sim1 neurons, likely acting as a neuromodulator, has a major role in the manifestation of anxiety-like behaviors. This may have important implications for how to best target CRH expression or action as a potential therapeutic approach to the clinical treatment of anxiety disorders in humans.

Validation of Crh floxed mice to create selective *Crh* deficiency

We first showed that the *Crh*flox mouse we created by flanking the second, coding exon of *Crh* with LoxP sites is functionally capable of selectively deleting *Crh*. We deleted *Crh* in gametes to create global *Crh*KO mice by crossing *Crh*flox mice with *EIIa*Cre mice, in which Cre is expressed in the early mouse embryo.[49] By this method we obtained germline homozygous Crh-deficient mice that completely recapitulated the phenotype of the *Crh* knockout mice we had previously created by a different targeted *Crh* deletion strategy in a line of mixed 129/C57BL/6 background that retained expression of *Pgk*neo,[13] including neonatal lethal lung dysplasia when born from *Crh*-deficient homozygous mothers which is rescued by prenatal glucocorticoid therapy,[50] absence of Crh peptide and mRNA from brain, atrophic adrenal glands with preserved adrenomedullary tissue, markedly attenuated basal diurnal corticosterone secretion,[51] and severely attenuated stimulated corticosterone following restraint stress.[52] These actions of Crh in mice are mediated by Crhr1, global knockout of which phenocopies the neuroendocrine deficits of *Crh*KO mice.[17, 18] Deletion of *Crh* specifically in Sim1 neurons does not cause as profound a reduction in basal or stress-induced plasma corticosterone concentrations as does global deletion of *Crh*, possibly because *Sim1*Cre may not delete all PVH *Crh*. Supporting this, 1) Crh mRNA in the PVH region of *Sim1Crh*KO mice was reduced by 70–80% measured by in situ hybridization, by 60~70% in PVH-enriched hypothalamic punches measured by Q-RT-PCR (Fig. 2g,h), but only by 30% in whole hypothalamus (Fig. S4), and 2) Crh peptide was absent from the PVH but detectable in some neurons lateral to the PVH in *Sim1Crh*KO mice (Fig. 2j).

Contribution of PVH Crh to anxiety-like behaviors

The reduced anxiety phenotype of *Sim1Crh*KO mice is very similar to the behavior of *Crhr1* knockout mice,[17, 18] likely because this receptor transduces these Crh-mediated behaviors, a conclusion also supported by the ability of Crhr1-specific antagonists to reverse anxiety-like behaviors,[53] including, surprisingly, in *Crh*KO mice.[14] The observed anxiolytic behaviors in *Sim1Crh*KO mice are due neither to the presence of *Sim1*Cre nor to reduced plasma corticosterone, and are consistent with the existence of a PVHCrh-specific anxiogenic pathway. This conclusion is supported by findings in mice with postnatal deletion of *Pomc*, which have elevated hypothalamic *Crh* mRNA, markedly reduced plasma corticosterone, and a robust increase in anxiety-like behaviors.[54]

The different anxiety phenotypes observed between *Sim1Crh*KO and previous global *Crh*KO mice[13] suggest that a difference in the method, extent, or timing of *Crh* gene deletion may affect these behaviors. One difference between the two models is that only exon 2 (which includes the entire coding region) of *Crh* is deleted in *Sim1Crh*KO mice, whereas all of exon 1 and only the coding portion of exon 2 is deleted in the global *Crh*KO mouse.[55] Also, in the first,[13] but not in *Sim1Crh*KO mice, the phosphoglycerine kinase promoter, *Pgk*, drives expression of the neomycin resistance gene, *neo*, in most cells. Further, the behavioral studies in the global *Crh*KO mouse were performed in mice on a mixed 129/C57BL/6 background,[17, 18] whereas *Sim1Crh*KO mice are on a pure C57BL/6 background. Finally, *Sim1Crh*KO mice manifest *Crh* deficiency only after e10.5, when Sim1 expression in mouse brain is first detected,[24] whereas global *Crh* knockout mice lack *Crh* from the time of

conception. The earlier deletion in global *Crh*KO mice might trigger different compensatory processes, such as urocortin being able to substitute for the loss of Crh.[53]

The target neurons responsible for reduced anxiety in *Sim1Crh*KO mice are not known. Using Crh-ires-Cre/AAV reporter mice, we found that cerebral cortex, BNST, septum, amygdala, dorsolateral hypothalamus, NTS and LC receive efferent fiber projections from PVHCrh neurons. It is possible that PVHCrh might evoke stress-induced behavioral responses via these pathways, since the BNST receives information from stress-regulatory limbic regions,[56–58] and the amygdala mediates responses to stress by altering hindbrain neuroendocrine, autonomic and behavioral pathways.[59] Although the amygdala is a behavioral target for glucocorticoids,[9–11, 60–62] we consider it unlikely that reduced corticosterone in *Sim1Crh*KO mice causes their anxiolytic behavior, since corticosterone supplementation does not reverse it. PVHCrh neurons project to NTS and LC and other regions of the caudal brainstem and spinal cord, such that if autonomic responses to stress were blunted in *Sim1Crh*KO mice, decreased interoceptive transmission could contribute to reduced anxiety behaviors. We could not answer whether *Sim1Crh*KO mice have reduced Crh autonomic projections using Crh-ires-Cre/AAV reporter mice (which express Crh in all its endogenous sites), but we did not observe any reduction in Crh mRNA expression in the brainstem of Sim1CrhKO animals.

Anxiety disorders are among the most common of all psychiatric diseases.[63] Although a link between CRH and anxiety is less clear in humans than in animals, compelling data exist.[45] Single nucleotide polymorphisms (SNPs) in *CRH* and *CRHR1* are associated with phenotypes linked to anxiety,[64] depression,[65, 66] and anti-depressant treatment responses.[67, 68] Postmortem studies of depressed persons reveal increased numbers of CRH-expressing neurons in the hypothalamus,[69] decreased CRH binding in frontal cortex,[70] and increased CRH content of cerebral spinal fluid.[71] Nonetheless, of the eight completed phase II and III drug trials of CRHR1 nonpeptide antagonists in subjects with either depression or anxiety, six have been largely negative[72–75] and findings of the other two have not been disclosed.[45] How can our results in *Sim1Crh*KO mice be reconciled with these negative CRHR1 antagonist trial outcomes? Griebel and Holsboer have offered several plausible explanations ranging from the preclinical use of inappropriate animal models to the clinical phase II/III use of heterogeneous trial subjects.[45] We offer another explanation based upon the anxiolytic effect of selective Crh deficiency in *Sim1Crh*KO mice. Rather than targeting CRH receptors throughout the brain, perhaps more focused inhibition of CRH production or release from neurons that co-express CRH and SIM1 would be more effective in the treatment of anxiety and depression disorders. Although this will be technically challenging, CRH originating in SIM1 neurons may be a promising therapeutic target for the treatment of psychiatric diseases.

Supplementary Material

Refer to Web version on PubMed Central for supplementary material.

Acknowledgments

We thank Drs. Clifford B. Saper and Nick Andrews for their helpful discussion. We acknowledge the BCH Neurodevelopmental Behavior Core (IDDRC, P30 HD 18655) and the Rodent Histopathology Core lab, Harvard Medical School for their technical support. We thank Dr. Bradford Lowell for the kind gift of Crh-ires-Cre mice. This study was supported by National Institutes of Health Grants 5K01MH096148-03 (to R.Z), T32DK007699-30 (to J.A.M), and NSFC 31271095 (to R.Z.).

References

1. McEwen BS. Central effects of stress hormones in health and disease: Understanding the protective and damaging effects of stress and stress mediators. European journal of pharmacology. 2008; 583(2–3):174–185. [PubMed: 18282566]
2. Toth M, Gresack JE, Bangasser DA, Plona Z, Valentino RJ, Flandreau EI, et al. Forebrain-specific CRF overproduction during development is sufficient to induce enduring anxiety and startle abnormalities in adult mice. Neuropsychopharmacology. 2014; 39(6):1409–1419. [PubMed: 24326400]
3. Bale TL, Vale WW. CRF and CRF receptors: role in stress responsivity and other behaviors. Annu Rev Pharmacol Toxicol. 2004; 44:525–557. [PubMed: 14744257]
4. McEwen BS. Physiology and neurobiology of stress and adaptation: central role of the brain. Physiol Rev. 2007; 87(3):873–904. [PubMed: 17615391]
5. Dallman MF. Modulation of stress responses: how we cope with excess glucocorticoids. Exp Neurol. 2007; 206(2):179–182. [PubMed: 17628543]
6. Vale W, Spiess J, Rivier C, Rivier J. Characterization of a 41-residue ovine hypothalamic peptide that stimulates secretion of corticotropin and beta-endorphin. Science. 1981; 213(4514):1394–1397. [PubMed: 6267699]
7. Widmaier EP, Dallman MF. The effects of corticotropin-releasing factor on adrenocorticotropin secretion from perifused pituitaries in vitro: rapid inhibition by glucocorticoids. Endocrinology. 1984; 115(6):2368–2374. [PubMed: 6094157]
8. Bao AM, Swaab DF. Corticotropin-releasing hormone and arginine vasopressin in depression focus on the human postmortem hypothalamus. Vitam Horm. 2010; 82:339–365. [PubMed: 20472147]
9. Choleris E, Devidze N, Kavaliers M, Pfaff DW. Steroidal/neuropeptide interactions in hypothalamus and amygdala related to social anxiety. Prog Brain Res. 2008; 170:291–303. [PubMed: 18655890]
10. Rodrigues SM, LeDoux JE, Sapolsky RM. The influence of stress hormones on fear circuitry. Annu Rev Neurosci. 2009; 32:289–313. [PubMed: 19400714]
11. Arnett MG, Kolber BJ, Boyle MP, Muglia LJ. Behavioral insights from mouse models of forebrain–and amygdala-specific glucocorticoid receptor genetic disruption. Mol Cell Endocrinol. 2011; 336(1–2):2–5. [PubMed: 21094675]
12. Finn DA, Rutledge-Gorman MT, Crabbe JC. Genetic animal models of anxiety. Neurogenetics. 2003; 4(3):109–135. [PubMed: 12687420]
13. Muglia L, Jacobson L, Dikkes P, Majzoub JA. Corticotropin-releasing hormone deficiency reveals major fetal but not adult glucocorticoid need. Nature. 1995; 373(6513):427–432. [PubMed: 7830793]
14. Weninger SC, Dunn AJ, Muglia LJ, Dikkes P, Miczek KA, Swiergiel AH, et al. Stress-induced behaviors require the corticotropin-releasing hormone (CRH) receptor, but not CRH. Proc Natl Acad Sci U S A. 1999; 96(14):8283–8288. [PubMed: 10393986]
15. Dunn AJ, Swiergiel AH. Behavioral responses to stress are intact in CRF-deficient mice. Brain Res. 1999; 845(1):14–20. [PubMed: 10529439]
16. van Gaalen MM, Stenzel-Poore MP, Holsboer F, Steckler T. Effects of transgenic overproduction of CRH on anxiety-like behaviour. Eur J Neurosci. 2002; 15(12):2007–2015. [PubMed: 12099906]
17. Smith GW, Aubry JM, Dellu F, Contarino A, Bilezikjian LM, Gold LH, et al. Corticotropin releasing factor receptor 1-deficient mice display decreased anxiety, impaired stress response, and aberrant neuroendocrine development. Neuron. 1998; 20(6):1093–1102. [PubMed: 9655498]

18. Timpl P, Spanagel R, Sillaber I, Kresse A, Reul JM, Stalla GK, et al. Impaired stress response and reduced anxiety in mice lacking a functional corticotropin-releasing hormone receptor 1. Nat Genet. 1998; 19(2):162–166. [PubMed: 9620773]
19. Bale TL, Contarino A, Smith GW, Chan R, Gold LH, Sawchenko PE, et al. Mice deficient for corticotropin-releasing hormone receptor-2 display anxiety-like behaviour and are hypersensitive to stress. Nature genetics. 2000; 24(4):410–414. [PubMed: 10742108]
20. Kita I, Seki Y, Nakatani Y, Fumoto M, Oguri M, Sato-Suzuki I, et al. Corticotropin-releasing factor neurons in the hypothalamic paraventricular nucleus are involved in arousal/yawning response of rats. Behavioural brain research. 2006; 169(1):48–56. [PubMed: 16413065]
21. Rodaros D, Caruana DA, Amir S, Stewart J. Corticotropin-releasing factor projections from limbic forebrain and paraventricular nucleus of the hypothalamus to the region of the ventral tegmental area. Neuroscience. 2007; 150(1):8–13. [PubMed: 17961928]
22. Hsu DT, Price JL. Paraventricular thalamic nucleus: subcortical connections and innervation by serotonin, orexin, and corticotropin-releasing hormone in macaque monkeys. The Journal of comparative neurology. 2009; 512(6):825–848. [PubMed: 19085970]
23. Balthasar N, Dalgaard LT, Lee CE, Yu J, Funahashi H, Williams T, et al. Divergence of melanocortin pathways in the control of food intake and energy expenditure. Cell. 2005; 123(3): 493–505. [PubMed: 16269339]
24. Fan CM, Kuwana E, Bulfone A, Fletcher CF, Copeland NG, Jenkins NA, et al. Expression patterns of two murine homologs of Drosophila single-minded suggest possible roles in embryonic patterning and in the pathogenesis of Down syndrome. Molecular and cellular neurosciences. 1996; 7(1):1–16. [PubMed: 8812055]
25. Liu P, Jenkins NA, Copeland NG. A highly efficient recombineering-based method for generating conditional knockout mutations. Genome Res. 2003; 13(3):476–484. [PubMed: 12618378]
26. Vahl TP, Ulrich-Lai YM, Ostrander MM, Dolgas CM, Elfers EE, Seeley RJ, et al. Comparative analysis of ACTH and corticosterone sampling methods in rats. Am J Physiol Endocrinol Metab. 2005; 289(5):E823–828. [PubMed: 15956051]
27. Rogers DC, Fisher EM, Brown SD, Peters J, Hunter AJ, Martin JE. Behavioral and functional analysis of mouse phenotype: SHIRPA, a proposed protocol for comprehensive phenotype assessment. Mamm Genome. 1997; 8(10):711–713. [PubMed: 9321461]
28. Solomon MB, Furay AR, Jones K, Packard AE, Packard BA, Wulsin AC, et al. Deletion of forebrain glucocorticoid receptors impairs neuroendocrine stress responses and induces depression-like behavior in males but not females. Neuroscience. 2012; 203:135–143. [PubMed: 22206943]
29. Marriott AS, Smith EF. An analysis of drug effects in mice exposed to a simple novel environment. Psychopharmacologia. 1972; 24(3):397–406. [PubMed: 5034940]
30. Boissier JR, Simon P. The exploration reaction in the mouse Preliminary note. Therapie. 1962; 17:1225–1232. [PubMed: 13968530]
31. Pellow S, Chopin P, File SE, Briley M. Validation of open:closed arm entries in an elevated plus-maze as a measure of anxiety in the rat. J Neurosci Methods. 1985; 14(3):149–167. [PubMed: 2864480]
32. Crawley J, Goodwin FK. Preliminary report of a simple animal behavior model for the anxiolytic effects of benzodiazepines. Pharmacol Biochem Behav. 1980; 13(2):167–170.
33. Bevins RA, Besheer J, Palmatier MI, Jensen HC, Pickett KS, Eurek S. Novel-object place conditioning: behavioral and dopaminergic processes in expression of novelty reward. Behav Brain Res. 2002; 129(1–2):41–50. [PubMed: 11809493]
34. Ennaceur A, Michalikova S, Bradford A, Ahmed S. Detailed analysis of the behavior of Lister and Wistar rats in anxiety, object recognition and object location tasks. Behav Brain Res. 2005; 159(2): 247–266. [PubMed: 15817188]
35. Silvers JM, Harrod SB, Mactutus CF, Booze RM. Automation of the novel object recognition task for use in adolescent rats. J Neurosci Methods. 2007; 166(1):99–103. [PubMed: 17719091]
36. Kutlu MG, Gould TJ. Nicotine modulation of fear memories and anxiety: Implications for learning and anxiety disorders. Biochem Pharmacol. 2015; 97(4):498–511. [PubMed: 26231942]

37. Zhang R, Jankord R, Flak JN, Solomon MB, D'Alessio DA, Herman JP. Role of glucocorticoids in tuning hindbrain stress integration. J Neurosci. 2010; 30(44):14907–14914. [PubMed: 21048149]
38. Asai M, Ramachandrappa S, Joachim M, Shen Y, Zhang R, Nuthalapati N, et al. Loss of function of the melanocortin 2 receptor accessory protein 2 is associated with mammalian obesity. Science. 2013; 341(6143):275–278. [PubMed: 23869016]
39. Paxinos G, Franklin K. The mouse brain. Elsevier. 2012
40. Huo L, Grill HJ, Bjorbaek C. Divergent regulation of proopiomelanocortin neurons by leptin in the nucleus of the solitary tract and in the arcuate hypothalamic nucleus. Diabetes. 2006; 55(3):567–573. [PubMed: 16505217]
41. Munzberg H, Flier JS, Bjorbaek C. Region-specific leptin resistance within the hypothalamus of diet-induced obese mice. Endocrinology. 2004; 145(11):4880–4889. [PubMed: 15271881]
42. Rozen S, Skaletsky H. Primer3 on the WWW for general users and for biologist programmers. Methods Mol Biol. 2000; 132:365–386. [PubMed: 10547847]
43. Livak KJ, Schmittgen TD. Analysis of relative gene expression data using real-time quantitative PCR and the 2(-Delta Delta C(T)) Method. Methods. 2001; 25(4):402–408. [PubMed: 11846609]
44. Krashes MJ, Shah BP, Madara JC, Olson DP, Strochlic DE, Garfield AS, et al. An excitatory paraventricular nucleus to AgRP neuron circuit that drives hunger. Nature. 2014; 507(7491):238–242. [PubMed: 24487620]
45. Griebel G, Holsboer F. Neuropeptide receptor ligands as drugs for psychiatric diseases: the end of the beginning? Nat Rev Drug Discov. 2012; 11(6):462–478. [PubMed: 22596253]
46. Oades RD, Isaacson RL. The development of food search behavior by rats: the effects of hippocampal damage and haloperidol. Behav Biol. 1978; 24(3):327–337. [PubMed: 743067]
47. Christmas AJ, Maxwell DR. A comparison of the effects of some benzodiazepines and other drugs on aggressive and exploratory behaviour in mice and rats. Neuropharmacology. 1970; 9(1):17–29. [PubMed: 5464000]
48. Crawley, J. What's Wrong With My Mouse?: Behavioral Phenotyping of Transgenic and Knockout Mice. 2nd. Wiley-Liss; 2007.
49. Lakso M, Pichel JG, Gorman JR, Sauer B, Okamoto Y, Lee E, et al. Efficient in vivo manipulation of mouse genomic sequences at the zygote stage. Proc Natl Acad Sci U S A. 1996; 93(12):5860–5865. [PubMed: 8650183]
50. Muglia LJ, Bae DS, Brown TT, Vogt SK, Alvarez JG, Sunday ME, et al. Proliferation and differentiation defects during lung development in corticotropin-releasing hormone-deficient mice. Am J Respir Cell Mol Biol. 1999; 20(2):181–188. [PubMed: 9922208]
51. Muglia LJ, Jacobson L, Weninger SC, Luedke CE, Bae DS, Jeong KH, et al. Impaired diurnal adrenal rhythmicity restored by constant infusion of corticotropin-releasing hormone in corticotropin-releasing hormone-deficient mice. J Clin Invest. 1997; 99(12):2923–2929. [PubMed: 9185516]
52. Jacobson L, Muglia LJ, Weninger SC, Pacak K, Majzoub JA. CRH deficiency impairs but does not block pituitary-adrenal responses to diverse stressors. Neuroendocrinology. 2000; 71(2):79–87. [PubMed: 10686522]
53. Waters RP, Rivalan M, Bangasser DA, Deussing JM, Ising M, Wood SK, et al. Evidence for the role of corticotropin-releasing factor in major depressive disorder. Neurosci Biobehav Rev. 2015; 58:63–78. [PubMed: 26271720]
54. Greenman Y, Kuperman Y, Drori Y, Asa SL, Navon I, Forkosh O, et al. Postnatal ablation of POMC neurons induces an obese phenotype characterized by decreased food intake and enhanced anxiety-like behavior. Mol Endocrinol. 2013; 27(7):1091–1102. [PubMed: 23676213]
55. Muglia LJ, Jenkins NA, Gilbert DJ, Copeland NG, Majzoub JA. Expression of the mouse corticotropin-releasing hormone gene in vivo and targeted inactivation in embryonic stem cells. J Clin Invest. 1994; 93(5):2066–2072. [PubMed: 8182138]
56. Geerling JC, Shin JW, Chimenti PC, Loewy AD. Paraventricular hypothalamic nucleus: axonal projections to the brainstem. J Comp Neurol. 2010; 518(9):1460–1499. [PubMed: 20187136]
57. Cullinan WE, Herman JP, Watson SJ. Ventral subicular interaction with the hypothalamic paraventricular nucleus: evidence for a relay in the bed nucleus of the stria terminalis. J Comp Neurol. 1993; 332(1):1–20. [PubMed: 7685778]

58. Dong HW, Petrovich GD, Watts AG, Swanson LW. Basic organization of projections from the oval and fusiform nuclei of the bed nuclei of the stria terminalis in adult rat brain. J Comp Neurol. 2001; 436(4):430–455. [PubMed: 11447588]
59. Rinaman L. Hindbrain noradrenergic A2 neurons: diverse roles in autonomic, endocrine, cognitive, and behavioral functions. Am J Physiol Regul Integr Comp Physiol. 2011; 300(2):R222–235. [PubMed: 20962208]
60. Ahima RS, Harlan RE. Charting of type II glucocorticoid receptor-like immunoreactivity in the rat central nervous system. Neuroscience. 1990; 39(3):579–604. [PubMed: 1711170]
61. Fuxe K, Agnati LF. Receptor-receptor interactions in the central nervous system. A new integrative mechanism in synapses. Med Res Rev. 1985; 5(4):441–482. [PubMed: 2999530]
62. Makino S, Gold PW, Schulkin J. Corticosterone effects on corticotropin-releasing hormone mRNA in the central nucleus of the amygdala and the parvocellular region of the paraventricular nucleus of the hypothalamus. Brain Res. 1994; 640(1–2):105–112. [PubMed: 8004437]
63. Kessler RC, Chiu WT, Demler O, Merikangas KR, Walters EE. Prevalence, severity, and comorbidity of 12-month DSM-IV disorders in the National Comorbidity Survey Replication. Arch Gen Psychiatry. 2005; 62(6):617–627. [PubMed: 15939839]
64. Smoller JW, Rosenbaum JF, Biederman J, Kennedy J, Dai D, Racette SR, et al. Association of a genetic marker at the corticotropin-releasing hormone locus with behavioral inhibition. Biol Psychiatry. 2003; 54(12):1376–1381. [PubMed: 14675801]
65. Liu Z, Zhu F, Wang G, Xiao Z, Wang H, Tang J, et al. Association of corticotropin-releasing hormone receptor1 gene SNP and haplotype with major depression. Neurosci Lett. 2006; 404(3): 358–362. [PubMed: 16815632]
66. Polanczyk G, Caspi A, Williams B, Price TS, Danese A, Sugden K, et al. Protective effect of CRHR1 gene variants on the development of adult depression following childhood maltreatment: replication and extension. Arch Gen Psychiatry. 2009; 66(9):978–985. [PubMed: 19736354]
67. Licinio J, O'Kirwan F, Irizarry K, Merriman B, Thakur S, Jepson R, et al. Association of a corticotropin-releasing hormone receptor 1 haplotype and antidepressant treatment response in Mexican-Americans. Mol Psychiatry. 2004; 9(12):1075–1082. [PubMed: 15365580]
68. Papiol S, Arias B, Gasto C, Gutierrez B, Catalan R, Fananas L. Genetic variability at HPA axis in major depression and clinical response to antidepressant treatment. J Affect Disord. 2007; 104(1–3):83–90. [PubMed: 17467808]
69. Purba JS, Hoogendijk WJ, Hofman MA, Swaab DF. Increased number of vasopressin-and oxytocin-expressing neurons in the paraventricular nucleus of the hypothalamus in depression. Arch Gen Psychiatry. 1996; 53(2):137–143. [PubMed: 8629889]
70. Nemeroff CB, Owens MJ, Bissette G, Andorn AC, Stanley M. Reduced corticotropin releasing factor binding sites in the frontal cortex of suicide victims. Arch Gen Psychiatry. 1988; 45(6):577–579. [PubMed: 2837159]
71. Arato M, Banki CM, Bissette G, Nemeroff CB. Elevated CSF CRF in suicide victims. Biol Psychiatry. 1989; 25(3):355–359. [PubMed: 2536563]
72. Binneman B, Feltner D, Kolluri S, Shi Y, Qiu R, Stiger T. A 6-week randomized, placebo-controlled trial of CP-316,311 (a selective CRH1 antagonist) in the treatment of major depression. Am J Psychiatry. 2008; 165(5):617–620. [PubMed: 18413705]
73. Coric V, Feldman HH, Oren DA, Shekhar A, Pultz J, Dockens RC, et al. Multicenter, randomized, double-blind, active comparator and placebo-controlled trial of a corticotropin-releasing factor receptor-1 antagonist in generalized anxiety disorder. Depress Anxiety. 2010; 27(5):417–425. [PubMed: 20455246]
74. Kirchhoff VD, Nguyen HT, Soczynska JK, Woldeyohannes H, McIntyre RS. Discontinued psychiatric drugs in 2008. Expert Opin Investig Drugs. 2009; 18(10):1431–1443.
75. Zobel AW, Nickel T, Kunzel HE, Ackl N, Sonntag A, Ising M, et al. Effects of the high-affinity corticotropin-releasing hormone receptor 1 antagonist R121919 in major depression: the first 20 patients treated. J Psychiatr Res. 2000; 34(3):171–181. [PubMed: 10867111]

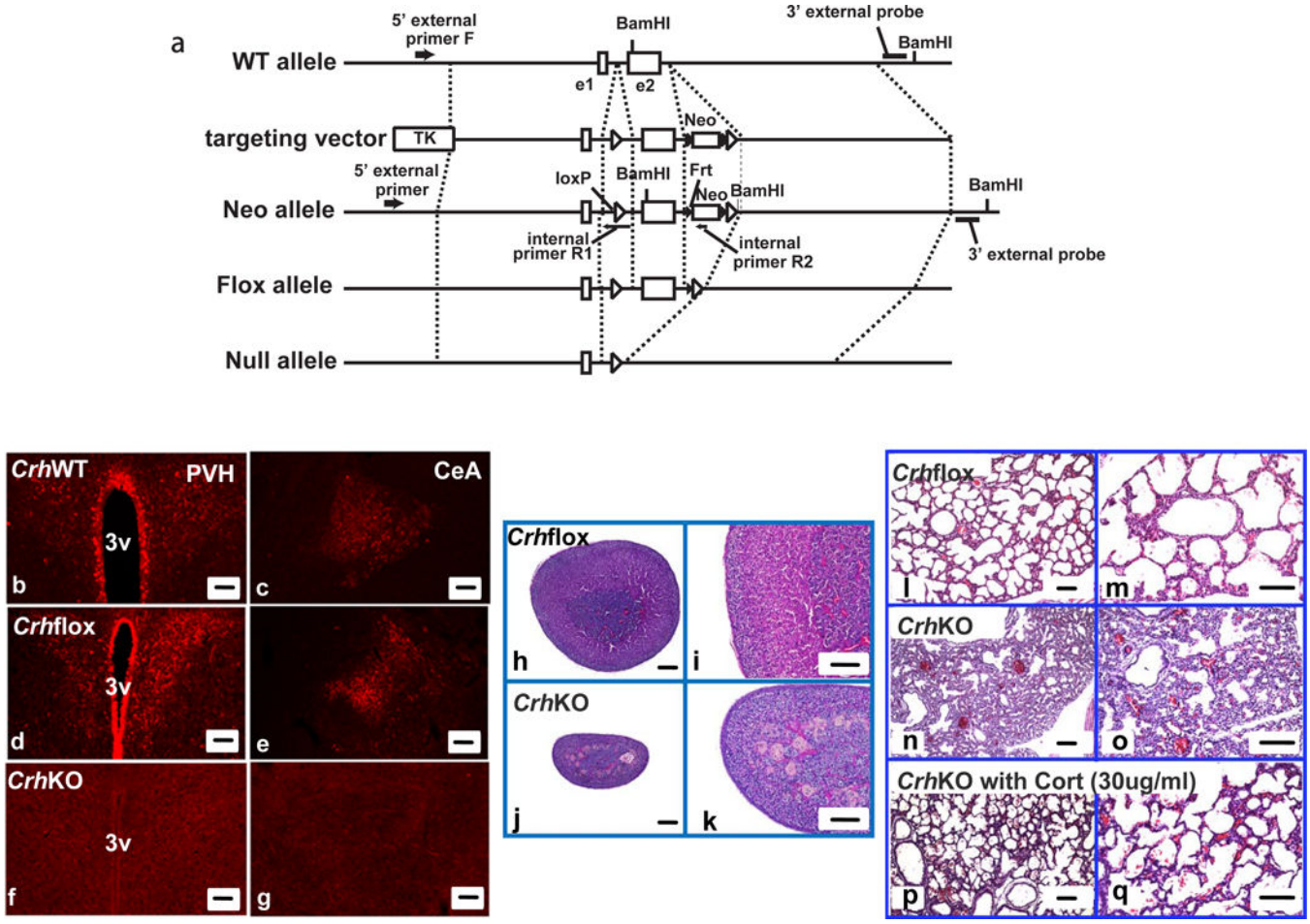

Figure 1.

Generation of *Crh*flox mouse and *Crh* null mouse (a). Schematic diagram of mouse *Crh* gene targeting. Wild-type (WT) *Crh* allele, targeting vector, Neo allele, flox allele, null allele are drawn. Broken lines indicate corresponding locations on each allele or the vector. The targeting vector has two artificial insertions, of which the upstream insertion contains one loxP sequence between exon1 (e1) and exon2 (e2), while the downstream insertion located downstream of exon2 contains the neomycin resistant gene (Neo) flanked by two frt sequences accompanied by an adjacent downstream loxP sequence. The location of two internal BamHI sites and one artificial BamHI site are indicated. Thymidine kinase (TK) is a negative selection marker. Characterization of *Crh*flox (*Crh*fl/fl) and *Crh*KO (*Crh*dl/dl) mice (b–q). (b–g) Crh-immuno-reactive neurons and fibers were observed in the paraventricular nucleus of hypothalamus (PVH) and central amygdala (CeA) in CrhWT (b, c) and *Crh*flox (d, e) but not in *Crh*KO mice (f, g) (scale bar, 100um); (h–k) Adrenal hypoplasia in *Crh*KO mice. Adrenals from adult male *Crh*flox (h, i) and *Crh*KO (j, k) were haematoxylin-eosin stained after paraformaldehyde fixation. *Crh*KO mice revealed thinner zona fasciculata. Left panel, low magnification (scale bar, 100um); right panel, high magnification (scale bar, 100um); (l–q) Confirmation of fetal lung dysplasia in *Crh*KO which was rescued by in utero corticosterone replacement. *Crh*flox fetus revealed normal lung development (l, m) while deletion of *Crh* cause hypercellular lungs with thick alveolar septae and a paucity of air

spaces (n, o). The deficiency of lung development was rescued by corticosterone administration (30ug/ml in drinking water) to female pregnant *Crh*KO mice (p, q). Left panel, low magnification (scale bar, 100um); right panel, high magnification (scale bar, 100um);

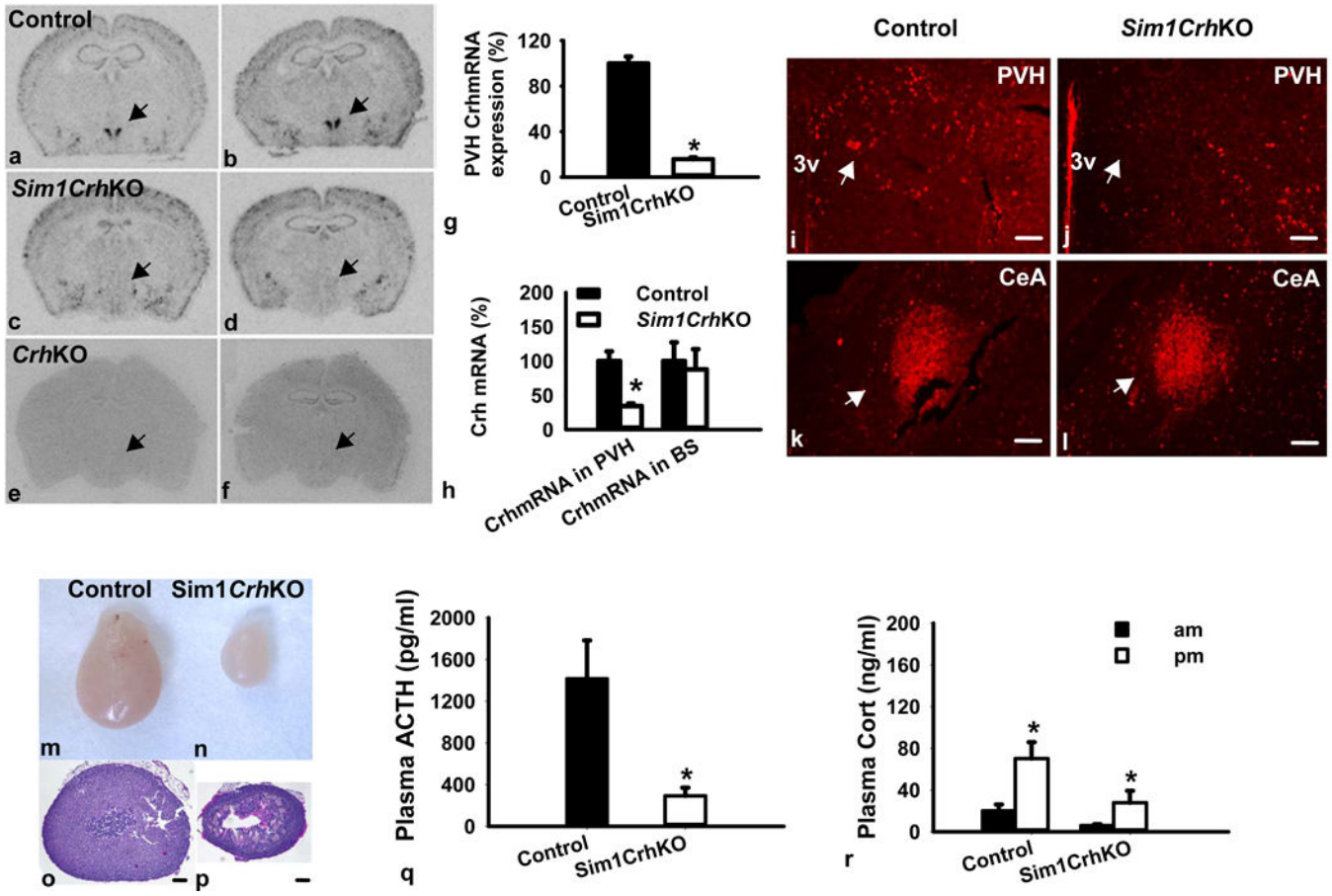

Figure 2.

Characterization of *Sim1Crh*KO mice. *Crh*flox mice were crossed with *Sim1*Cre mice to delete the floxed *Crh* gene in Sim1-expressing tissues; (a–f) Representative images for Crh mRNA expression in the PVH by in situ hybridization (Bregma −0.70mm to Bregma −1.06mm). Top row, *Crh*flox (control); middle row, *Sim1Crh*KO; bottom row, *Crh*KO. Arrows point to PVH; (g) Semi-quantitative densitometry of film images showed that Crh was deleted in the PVH area of *Sim1Crh*KO mice, (*Sim1Crh*KO versus *Crh*flox, n=8 versus 8); (h) Q RT-PCR analysis revealed that Crh mRNA expression decreased in the PVH but not in the brainstem in *Sim1Crh*KO mice compared to the control (*Sim1Crh*KO versus *Crh*flox, n=5 versus 4; Control, filled bars; *Sim1Crh*KO, open bars); (i–l) Crh immunohistochemistry staining in the PVH and CeA. *Sim1Crh*KO showed less Crh-ir positive neurons and fibers in the PVH but comparable amount of Crh-ir positive staining in CeA area. Arrows point to PVH and CeA, scale bar: 100um; PVH, paraventricular nucleus of the hypothalamus; CeA, central nucleus of the amygdala; (m–r) Physiological characterization of *Sim1Crh*KO mice; (m–p) Adrenal hypoplasia in *Sim1Crh*KO versus *Crh*flox control mice: Whole adrenals and haematoxylin-eosin stained adrenal sections from the widest diameter, respectively, of *Crh*flox (m, o) and *Sim1Crh*KO (n, p) male mice; (q) Plasma ACTH was lower in male *Sim1Crh*KO (7) versus *Crh*flox (10) mice; (r) Plasma corticosterone was lower in *Sim1Crh*KO versus *Crh*flox mice at diurnal morning (9–10am) and evening (5–6pm) in males (n = 7 versus 10); *p<0.05 versus control.

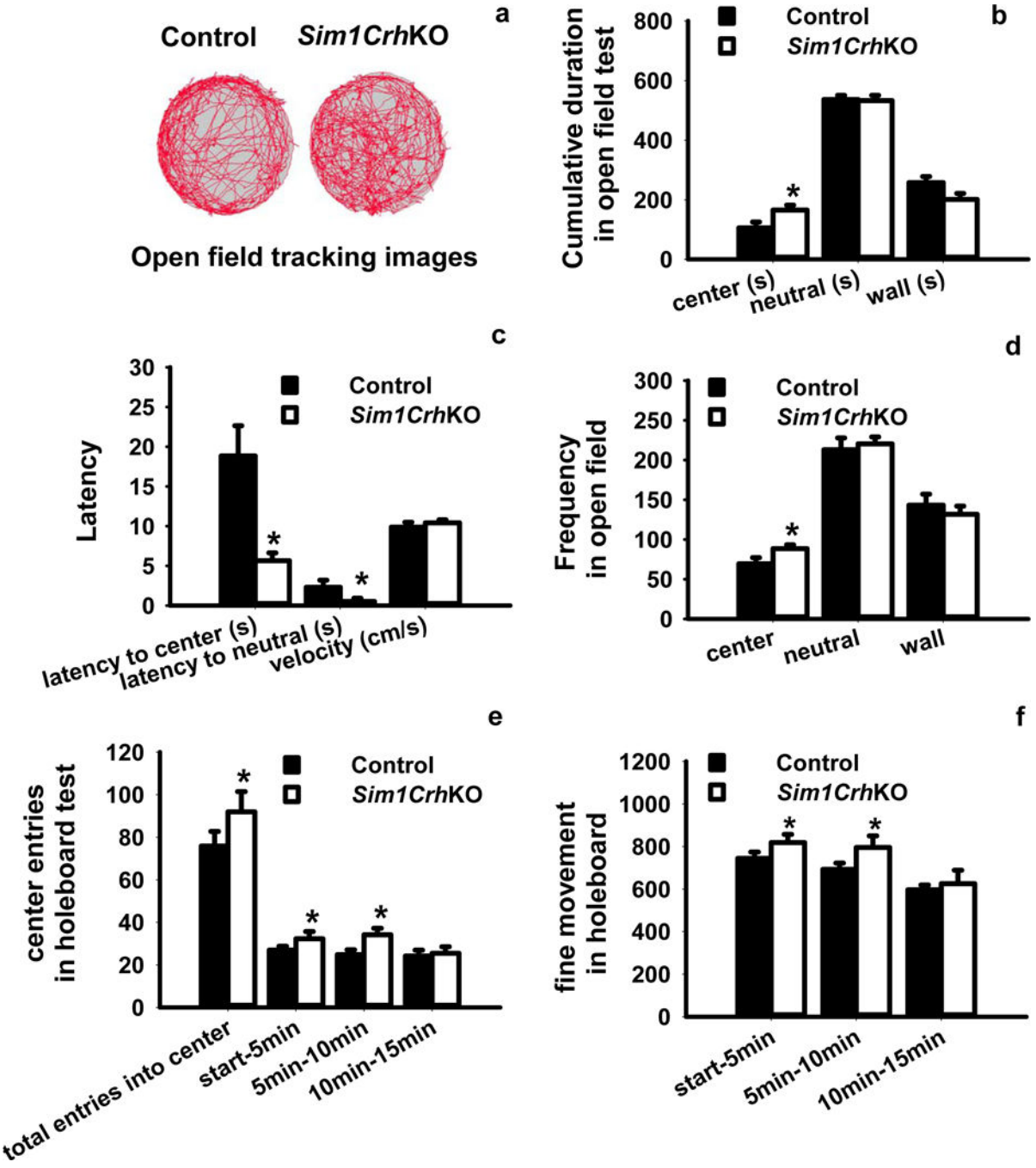

Figure 3.

Analysis of anxiety-like behaviors by the open field test and holeboard test. (a, b) Compared to *Crh*flox control mice, *Sim1Crh*KO mice spent more time in the center area and less time in wall areas while both groups spent equivalent amounts of time in neutral areas; c) *Sim1Crh*KO mice revealed decreased latency of first entry into center and neutral areas compared with control mice, whereas there were no differences for velocity; d) *Sim1Crh*KO mice entered into center more frequently compared to control animals; e) Holeboard analysis revealed *Sim1Crh*KO mice had significantly increased entrance frequency into the

center compared to *Crh*flox controls, and that this occurred during the first and second 5 minute periods; f) Fine movement was significantly increased in *Sim1Crh*KO compared to *Crh*flox mice. *P<0.05, *Sim1Crh*KO versus *Crh*flox control mice (n = 7 versus 10).

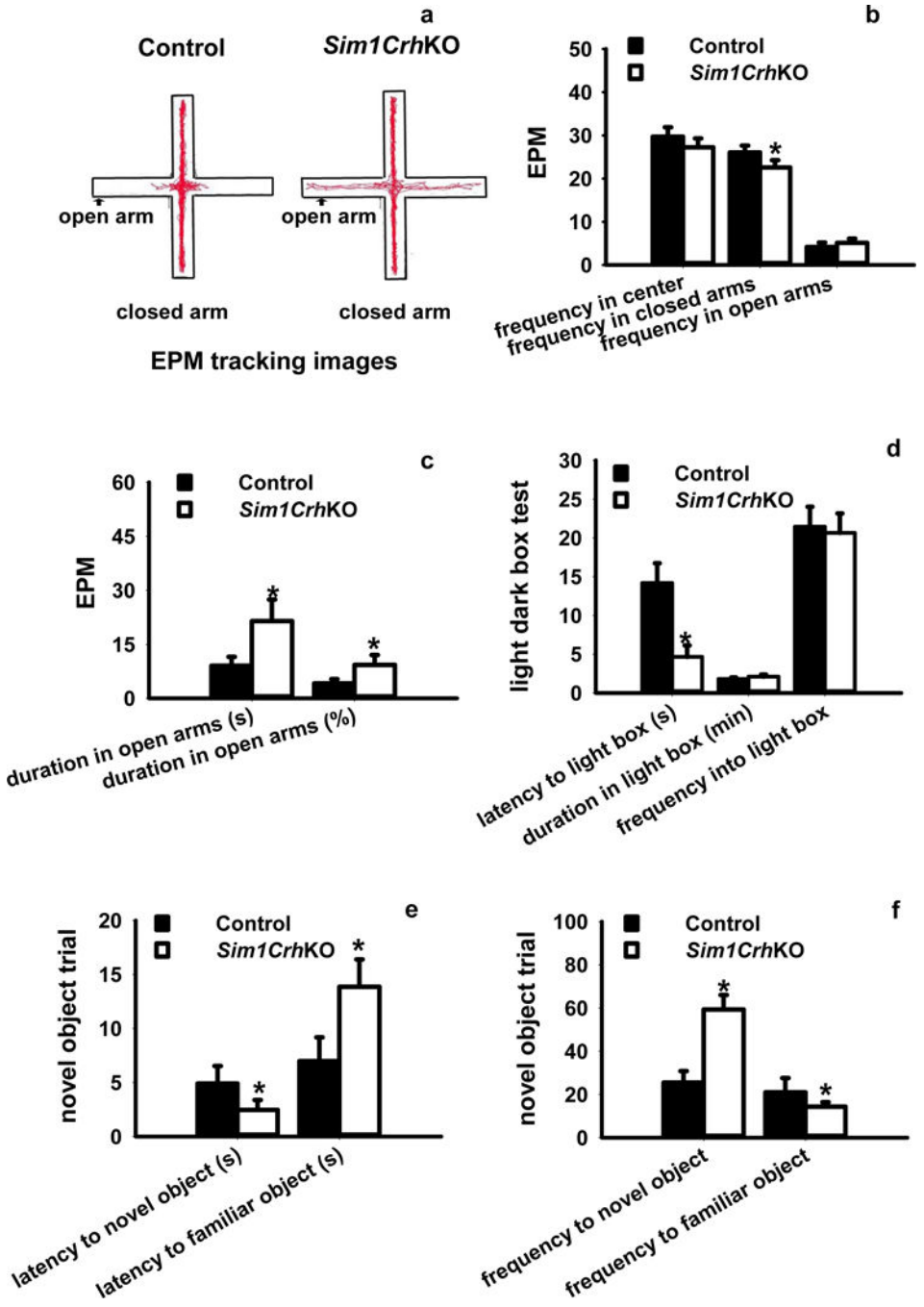

Figure 4.

Analysis of anxiety-like behaviors by the elevated plus maze (EPM), light-dark box and novel object recognition test (NORT). a, b) EPM analysis revealed that deletion of Crh in *Sim1*Cre neurons significantly decreased the entrance frequency into the closed arms compared to *Crh*flox control mice; c) *Sim1Crh*KO mice spent significantly more time in the open arms in term of duration and percentage compared to control mice; d) *Sim1Crh*KO compared with *Crh*flox mice had a shorter latency to emerge from darkness into the light box. However, there were no differences in other measured anxiety parameters (time spent in

the light part, frequency into light box. d) There were no significant differences for duration in center and closed arms between control and *Sim1Crh*KO mice; e) Deletion of Crh from Sim1 neurons significantly decreased latency to novel objects while increased latency to familiar objects; f) *Sim1Crh*KO mice exhibited significantly increased touching frequency for novel objects while decreased exploring behaviors for familiar objects; *P<0.05, *Sim1Crh*KO versus *Crh*flox control mice (n = 7 versus 10).

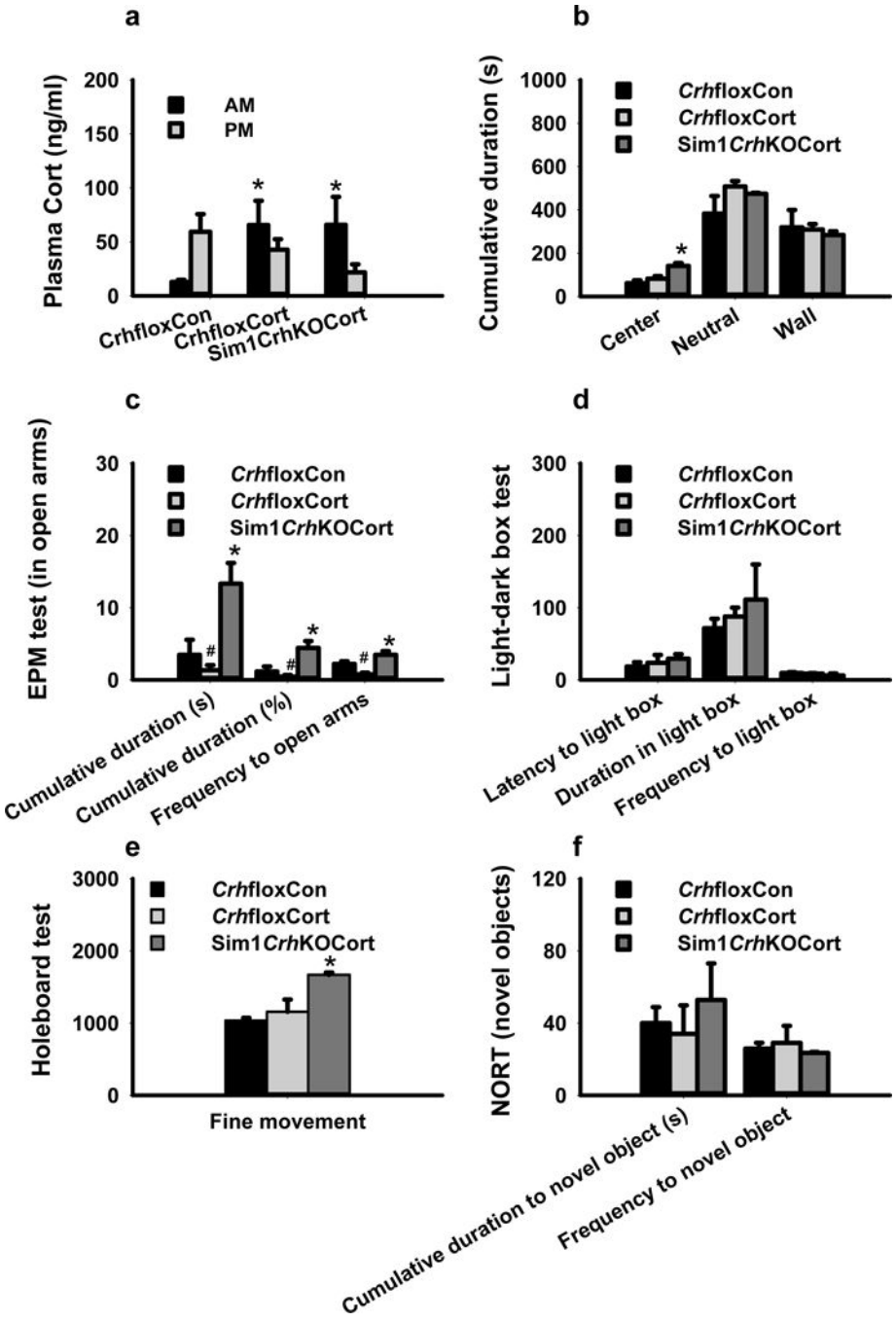

Figure 5.

Corticosterone supplementation did not reverse anxiolytic behaviors in *Sim1Crh*KO mice. a) Morning (7–8am) plasma corticosterone increased in *Crhflox*Cort and *Sim1Crh*KOCort animals during administration of corticosterone (5ug/ml) in drinking water compared to *Crhflox*Con mice; b) *Sim1Crh*KOCort mice spent more time in the center of open field test compared to *Crhflox*Con and *Crhflox*Cort mice; c) During EPM testing, *Sim1Crh*KO mice with corticosterone supplementation (*Sim1Crh*KOCort), had significantly increased cumulative duration and the entrance frequency into the open arms compared to *Crh*flox

control mice, while *Crh*floxCort animals had decreased time in the open arms; d) During lightbox testing, *Sim1Crh*KOCort mice showed a non-significant trend of more time in the light area; e) During holeboard testing, *Sim1Crh*KOCort mice showed increased fine movement compared to *Crhflox*Con and *Crhflox*Cort animals; f) During novel object testing, *Sim1Crh*KOCort mice showed a non-significant trend towards increased cumulative duration for novel objects; *P<0.05, *Sim1Crh*KOCort and *Crh*floxCort versus *Crh*floxCon; #P<0.05, *Crh*floxCort versus *Crh*floxCon. For all tests, *Sim1Crh*KOCort (n = 4), *Crh*floxCon (n = 5) and *Crh*floxCort (n = 4).